

## Exploring the influence of operational parameters on the reactivity of elemental iron materials

C. Noubactep<sup>a,\*</sup>, T. Licha<sup>a</sup>, T.B. Scott<sup>b</sup>, M. Fall<sup>c</sup>, M. Sauter<sup>a</sup>

<sup>a</sup> *Angewandte Geologie, Universität Göttingen, Goldschmidtstrasse 3, D-37077 Göttingen, Germany*

<sup>b</sup> *University of Bristol, Interface Analysis Centre, 121 St. Michael's Hill, Bristol BS2 8BS, UK*

<sup>c</sup> *University of Ottawa, Department of Civil Engineering, 161 Louis Pasteur, Ottawa, Ontario, Canada, K1N 6N5*

### ARTICLE INFO

#### Article history:

Received 16 April 2009

Received in revised form 20 July 2009

Accepted 21 July 2009

Available online 6 August 2009

#### Keywords:

EDTA

Electrochemical reactivity

Operational parameters

Water remediation

Zeravalent iron

### ABSTRACT

In an attempt to characterize material intrinsic reactivity, iron dissolution from elemental iron materials ( $\text{Fe}^0$ ) was investigated under various experimental conditions in batch tests. Dissolution experiments were performed in a dilute solution of ethylenediaminetetraacetate ( $\text{Na}_2\text{-EDTA} - 2 \text{ mM}$ ). The dissolution kinetics of 18  $\text{Fe}^0$  materials were investigated. The effects of individual operational parameters were assessed using selected materials. The effects of available reactive sites [ $\text{Fe}^0$  particle size ( $\leq 2.0 \text{ mm}$ ) and metal loading ( $2\text{--}64 \text{ g L}^{-1}$ )], mixing type (air bubbling, shaking), shaking intensity ( $0\text{--}250 \text{ min}^{-1}$ ), and  $\text{Fe}^0$  pre-treatment (ascorbate, HCl and EDTA washing) were investigated. The data were analysed using the initial dissolution rate ( $k_{\text{EDTA}}$ ). The results show increased iron dissolution with increasing reactive sites (decreasing particle size or increasing metal loading), and increasing mixing speed. Air bubbling and material pre-treatment also lead to increased iron dissolution. The main output of this work is that available results are hardly comparable as they were achieved under very different experimental conditions. A unified experimental procedure for the investigation of processes in  $\text{Fe}^0/\text{H}_2\text{O}$  systems is suitable. Alternatively, a parameter ( $\tau_{\text{EDTA}}$ ) is introduced which could routinely used to characterize  $\text{Fe}^0$  reactivity under given experimental conditions.

© 2009 Elsevier B.V. All rights reserved.

### 1. Introduction

Elemental iron ( $\text{Fe}^0$ ) is a well known material for the abiotic removal of organic and inorganic contaminants from groundwater, soils, sediments, and waste streams [1–14].  $\text{Fe}^0$  is widely termed in the literature on permeable reactive barriers as zerovalent iron (ZVI) and is available as  $\text{Fe}^0$ -based alloys ( $\text{Fe}^0$  materials), mostly cast iron and low alloy steel. Reduction through electron transfer from the body of the  $\text{Fe}^0$  (direct reduction) is currently considered as the main removal mechanism for the majority of contaminants in  $\text{Fe}^0/\text{H}_2\text{O}$  systems [4,9,15]. However, for this thermodynamic founded assumption to be realized, the  $\text{Fe}^0$  surface has to be accessible to the contaminant species. Alternatively, the surface must be covered by an electron conductive oxide-film (e.g.,  $\text{Fe}_3\text{O}_4$ ). In all cases, experiments are to be conducted under conditions which closely mimic those found in nature. In particular, mixing of the solution should neither delay nor prevent the formation of an oxide-film in the vicinity of the  $\text{Fe}^0$  surface [16,17]. This aspect of mixing has been mostly overseen since mixing is essentially used as a tool to accelerate contaminant transport to  $\text{Fe}^0$  surface [18,19].

This example illustrates the necessity of exploring and/or revisiting the influence of operational parameters on the processes of iron dissolution which is coupled to contaminant removal.

In the last 15 years a huge number of studies have been conducted with the aim to understand the impact of operational conditions on the processes of contaminant removal in  $\text{Fe}^0/\text{H}_2\text{O}$  systems [2,15,18,20–23]. The investigated experimental conditions included:  $\text{Fe}^0$  Characteristics,  $\text{Fe}^0$  type,  $\text{Fe}^0$  particle size, dissolved oxygen, contaminant concentration, solution chemistry (e.g., pH, dissolved ligands), chemical modification of the original material, mixing type, mixing intensity and material loading. In these studies, the influence of the operational conditions on the removal efficiency for the respective contaminants was reported to be theoretically expected and experimentally verified. For instance, while investigating the effects of mixing intensity ( $\text{min}^{-1}$ ) on nitrate removal by nanoscale  $\text{Fe}^0$ , Choe et al. [20] found out that for mixing intensities  $<40 \text{ min}^{-1}$   $\text{NO}_3^-$  removal is largely a mass transport-limited surface reaction, the reaction taking place at the  $\text{Fe}^0/\text{H}_2\text{O}$  interface. However, from open literature on corrosion it is known that under natural conditions (near-neutral pH, slowly flowing groundwater) such an interface does not exist due to the ubiquitous presence of iron oxide that coats the metal surface [24–27] and provides two interfaces;  $\text{Fe}^0/\text{Fe-oxide}$  and  $\text{Fe-oxide}/\text{H}_2\text{O}$ . The fact that at  $\text{pH} >4.5$  an iron surface is always covered with an oxide-

\* Corresponding author. Tel.: +49 551 39 3191; fax: +49 551 399379.  
E-mail address: [cnoubac@gwdg.de](mailto:cnoubac@gwdg.de) (C. Noubactep).

**Table 1**  
Some relevant reactions for the elucidation of the mechanism of ZVI dissolution. oxid. = oxidative, compl. = complexive.

Process	Reaction equation
Fe <sup>0</sup> oxidation	Fe <sup>0</sup> + 2H <sub>2</sub> O ⇒ Fe <sup>2+</sup> + H <sub>2</sub> + 2HO <sup>-</sup> (1)
Fe <sup>0</sup> oxidation	Fe <sup>0</sup> + ½O <sub>2</sub> + H <sub>2</sub> O ⇌ Fe <sup>2+</sup> + 2HO <sup>-</sup> (2)
Fe <sup>2+</sup> oxidation	2Fe <sup>2+</sup> + ½O <sub>2</sub> + H <sub>2</sub> O ⇌ 2Fe <sup>3+</sup> + 2HO <sup>-</sup> (3)
Fe <sup>2+</sup> complexation	Fe <sup>2+</sup> + EDTA ⇌ Fe(EDTA) <sup>2+</sup> (4)
Fe <sup>3+</sup> complexation	Fe <sup>3+</sup> + EDTA ⇌ Fe(EDTA) <sup>3+</sup> (5)
Fe(OH) <sub>3</sub> formation	2Fe <sup>2+</sup> + ½O <sub>2</sub> + 5H <sub>2</sub> O ⇌ 2Fe(OH) <sub>3</sub> + 4H <sup>+</sup> (6)
Fe(OH) <sub>3</sub> aging	Fe(OH) <sub>3</sub> ⇌ FeOOH(Fe <sub>3</sub> O <sub>4</sub> , Fe <sub>2</sub> O <sub>3</sub> ) (7)
FeOOH dissolution	FeOOH + EDTA + 3H <sup>+</sup> ⇌ Fe(EDTA) <sup>3+</sup> + 2H <sub>2</sub> O (8)

film has been recognized in the reactive wall literature [28–31]. For example Chen et al. [29] used a 50 mM ethylenediaminetetraacetate (EDTA) solution to avoid oxide-film formation in their investigations on trichloroethylene degradation by Fe<sup>0</sup>. Because the oxide-film is omnipresent at the Fe<sup>0</sup> surface, the interactions of any contaminant in Fe<sup>0</sup>/H<sub>2</sub>O systems will depend on the nature (composition, conductivity, porosity, thickness) of the formed film and the affinity of the contaminant for the film material. Therefore, it is suitable to characterize Fe<sup>0</sup> reactivity and the effects of operational conditions in systems exempt from in situ generated oxide-films [31]. As a strong iron complexing agent without redox properties EDTA has been used successfully for this purpose [32,33]. In these previous works [32,33], a positive correlation between the extend of uranium (VI) removal and the dissolution rates in 2 mM EDTA ( $k_{\text{EDTA}}$ ) was demonstrated for thirteen Fe<sup>0</sup> materials. Recent data on methylene blue discoloration by the same materials corroborated reported results [18].

The present study aims to assess the ability of various Fe<sup>0</sup> materials to release Fe (Fe<sup>II</sup>, Fe<sup>III</sup> species) into a 2 mM EDTA solution and to establish the response of selected Fe<sup>0</sup> materials to a relative wide range of experimental conditions. The effects of Fe<sup>0</sup> particle size ( $\leq 2.0$  mm) and metal loading (2–64 g L<sup>-1</sup>), mixing type (air bubbling, shaking), shaking intensity (0–250 min<sup>-1</sup>), and Fe<sup>0</sup> pretreatment (ascorbate, HCl and EDTA washing) on Fe dissolution in batch operation mode were investigated and the degree of influence of each examined experimental parameter is discussed.

## 2. Some relevant aspects of the “Fe<sup>0</sup>/EDTA/H<sub>2</sub>O” system

Dissolution studies are commonly used as a tool to characterize the reactivity (or stability) of geological materials [34–38]. Using this tool the oxidative dissolution of Fe<sup>0</sup> materials can be investigated at approximately neutral pH in order to simulate pH conditions characteristic of natural groundwaters [39]. Since the solubility of iron in this pH range is very low, EDTA can be used to sustain material dissolution [28,29,31]. Table 1 summarises some relevant reactions occurring in a “Fe<sup>0</sup>/EDTA/H<sub>2</sub>O” system. A very comprehensive review on the chemistry of the “Fe<sup>0</sup>/EDTA/H<sub>2</sub>O” system is given by Pierce et al. [31].

In this system, Fe<sup>0</sup> dissolution is an oxidative process mediated by water (Eq. (1)) or dissolved oxygen (Eq. (2)). The resultant Fe<sup>2+</sup> ions can be further oxidized to Fe<sup>3+</sup> by dissolved O<sub>2</sub> (Eq. (3)) or complexed by EDTA, yielding [Fe<sup>II</sup>(EDTA)] and [Fe<sup>III</sup>(EDTA)] complexes (Eqs. (4) and (5)). [Fe<sup>II</sup>(EDTA)] complexes are highly sensitive to dissolved oxygen, and oxidative transformation to more stable [Fe<sup>III</sup>(EDTA)] complexes is completed in less than 1 min [40,41]. Eqs. (6)–(8) illustrate the formation of corrosion products and their complexive dissolution by EDTA. Corrosion products are usually mixture of iron oxides (FeOOH, Fe<sub>2</sub>O<sub>3</sub>, Fe<sub>3</sub>O<sub>4</sub>); it is expected, that the kinetics of their EDTA dissolution will primarily depend on the crystalline structure of individual oxides [42].

The basic approach of this study is to exploit the differences in initial dissolution behaviour of Fe<sup>0</sup> materials in a dilute EDTA solu-

tion (2 mM) in order to characterize their intrinsic reactivity [32,33] and also to investigate the response of the system to changes in some relevant operational parameters. Using a metal loading of 10 g L<sup>-1</sup> previous works have shown that the dependence of the iron concentration on the elapsed time for the material termed ZVIO here was a linear function (Eq. (9)) for the first 72 h of the experiment [32,33]. In Eq. (9) [Fe]<sub>t</sub> is the total iron concentration at time *t* as defined by Eq. 10

$$[\text{Fe}]_t = k_{\text{EDTA}} t + b \quad (9)$$

$$[\text{Fe}]_t = [\text{Fe}^{\text{II}}]_t + [\text{Fe}^{\text{III}}]_t + [\text{Fe}^{\text{II}}(\text{EDTA})]_t + [\text{Fe}^{\text{III}}(\text{EDTA})]_t \quad (10)$$

The current study was targeted at identifying the time frame for which the linearity of Eq. (9) is assured for the systems “Fe<sup>0</sup> (2 g L<sup>-1</sup>)/EDTA (2 mM)”. For each ZVI material the linear dissolution function obtained from experiment can be used to characterize the individual reactivity, with the linear gradient ( $k_{\text{EDTA}}$  in Eq. (9)) representing the rate of iron dissolution ( $k_{\text{EDTA}}$ ) and the intercept ( $b$  in Eq. (9)) representing the iron concentration at *t*<sub>0</sub> (ideally zero;  $b = [\text{Fe}]_{t_0}$ ), and providing an estimation of the amount of possibly readily soluble atmospheric corrosion products on the material. Ideally, under given experimental conditions, Fe concentration increases continuously with time from 0 mg L<sup>-1</sup> at the start of the experiment (*t*<sub>0</sub> = 0) to 112 mg L<sup>-1</sup> (0.002 M) at saturation (*t*<sub>sat</sub> =  $\tau_{\text{EDTA}}$ ) when a 1:1 complexation of Fe and EDTA occurs. Thus,  $\tau_{\text{EDTA}}$  is an operative parameter which could allow the characterization of the reactivity of each Fe<sup>0</sup> under any experimental conditions [43].

An independent process involving Fe<sup>0</sup>, EDTA and molecular O<sub>2</sub> was developed by Noradoun et al. [44,45] and is currently further developed [46–48]. This process uses the “zerovalent iron, EDTA and air” system (ZEA system) to generate HO• radicals for contaminant oxidation. In this process, EDTA itself is degraded [46]. Moreover, Gylieue et al. [49] have recently used Fe<sup>0</sup> for aqueous quantitative removal of up to 100 mM EDTA. The removal mechanism included degradation by HO• radicals and co-precipitation with iron corrosion products. The results of Gylieue et al. [49] indicate that under the experimental conditions of this work, EDTA (2 mM) could be removed only by degradation since the Fe<sup>0</sup> reactivity characterization is limited to the pre-saturation phase (no precipitation). In total, recent works on the Fe<sup>0</sup>/EDTA/H<sub>2</sub>O system, clearly demonstrated that EDTA is a concurrent contaminant for in situ generated oxidative species and should be regarded as instable.

The present study can be seen as an investigation of the short-term kinetics of iron dissolution in ZEA systems while characterizing the effects of operational parameters on this process. Clearly, a well-documented methodology is used to characterize Fe<sup>0</sup> reactivity as influenced by operational parameters. In this method dissolved oxygen is a reactant and not a disturbing factor. Furthermore, since the investigations are limited to the initial phase of iron dissolution (forward dissolution), the possibility that EDTA alters the corrosion process is not likely to be determinant [31]. Theoretically, EDTA should not deplete during this initial reaction phase which is dominated by forward iron dissolution. The well-documented instability of Fe<sup>III</sup>-EDTA complexes (photodegradation) is the sole concern here [50].

## 3. Material and methods

### 3.1. Solutions

Based on previous works [32,33], a working EDTA solution of 0.002 M (or 2 mM) was used in this study (also see the discussion in the Supporting Information). The working-solution was obtained by one step dilution of a commercial 0.02 M standard from Baker JT<sup>®</sup> with Milli-Q purified water. A standard iron solution (1000 mg L<sup>-1</sup>)

from Baker JT<sup>®</sup> was used to calibrate the Spectrophotometer. All other chemicals used were of analytical grade. In preparation for spectrophotometric analysis ascorbic acid was used to reduce Fe<sup>III</sup>-EDTA in solution to Fe<sup>II</sup>-EDTA. 1,10 orthophenanthroline (ACROS Organics) was used as reagent for Fe<sup>II</sup> complexation prior to spectrophotometric determination. Other chemicals used in this study included Na<sub>2</sub>-EDTA, NaHCO<sub>3</sub>, L(+)-ascorbic acid, L-ascorbic acid sodium salt, and sodium citrate. The initial pH of the working EDTA solutions was 5.2 and increased to values above 8.0 as result of iron corrosion.

### 3.2. Fe<sup>0</sup> materials

A total of 18 ZVI materials (ZVI0 through ZVI17) were obtained from various sources, in different forms and grain sizes. The main characteristics of these materials including form, grain size and elemental composition are summarised in Tables S11 and S12 (Supporting Information). No information about manufacturing processes (e.g., raw material, heat treatment) was available to assist with subsequent data interpretation. It is well reported that the specific surface area (SSA) of iron materials is one of the predominant factors in controlling reactivity and is directly related to grain size [51–53]. The materials investigated in this study have a variety of different grain sizes (<80–9000 μm) with resultant differences in specific surface area, although exact values were not available or determined. However, it was not the objective of this study to investigate the impact of the specific surface area on the reactivity of these different materials, but rather to compare the reactivity of the materials in their typical state (and form) in which they might be used for field applications. Apart from samples ZVI0, ZVI7 and ZVI11, all materials were used for experiment in an 'as received' state. Samples ZVI0, ZVI7 and ZVI11 were crushed and sieved, with the grain size fraction between 1 mm and 2 mm selected for reaction.

### 3.3. Iron dissolution experiments

Three different types of batch experiments were conducted at room temperature (~22 °C) for experimental durations varying from 0.5 to 144 h. The types of experiment are described in more detail in the following section:

#### 3.3.1. Type 1 open systems

Iron dissolution was initiated by the addition of 0.1 g of each material to 50 mL of a 2 mM EDTA solution (2 g L<sup>-1</sup> ZVI). Each reaction was run for ≤144 h (6 days) in triplicate using narrow 70 mL glass beakers to hold the solutions. The reacting samples were left undisturbed on the laboratory bench for the duration of experimental period and were shielded from direct sunlight to minimize Fe<sup>III</sup>-EDTA photodegradation [50]. These open systems (type 1) were used to characterize: (i) the reactivity of all used Fe<sup>0</sup> ( $k_{\text{EDTA}}$ ,  $b$  and  $\tau_{\text{EDTA}}$  values), and (ii) the effects of particle size and mass loading.

#### 3.3.2. Type 2 open systems

Dissolution was initiated by the addition of 0.2 g Fe<sup>0</sup> material in a sealed vessel containing 100 mL of EDTA solution (2 g L<sup>-1</sup> ZVI). Experiments were conducted for ≤96 h (4 days) in specially manufactured glass reaction vessels (~125 mL capacity) designed to allow continual mixing of the EDTA solution using a current of humid air supplied by a small aquaristic pump. The setup was designed to homogenize the experimental solutions at atmospheric pressure while keeping Fe<sup>0</sup> materials immobile at the bottom of the vessels. Experiments in type 2 open systems were performed to investigate the impact of mixing art on the process of Fe<sup>0</sup> dissolution. Parallel experiments (non-shaken, ultrasound) were

performed in the same vessels to account for possible influence of the reactor geometry.

#### 3.3.3. Closed systems

For each dissolution reaction 0.2 g of the Fe<sup>0</sup> material was added to 100 mL EDTA solution (2 g L<sup>-1</sup> ZVI) in sealed polypropylene Erlenmeyer flasks (Nalgene<sup>®</sup>). Each reaction was run for ≤96 h (4 days) in triplicate. For each experiment the Erlenmeyers were placed on a rotary shaker or in an ultrasonic bath and allowed to react. The shaking intensities used for different samples were 0, 50, 150, 200 and 250 min<sup>-1</sup>. Closed systems were performed to investigate the effects of mixing intensity.

At various time intervals, 0.100–1.000 mL (100–1000 μL) of the solution (non-filtrated) were withdrawn from the Erlenmeyer flask with a precision micro-pipette and diluted with distilled water to 10 mL (test solution) in 20 mL glass assay tubes in preparation for analysis. After each sampling the equivalent amount of distilled water was added back into the Erlenmeyer in order to maintain a constant volume.

### 3.4. Analytical method

The aqueous iron concentration was determined with a Varian Cary 50 UV–vis spectrophotometer, using a wavelength of 510 nm and following the 1,10 orthophenanthroline method [54,55]. The instrument was calibrated for iron concentration ≤10 mg L<sup>-1</sup>.

The pH value of each sample was measured by combination glass electrodes, that were pre-calibrated with five standards following a multi-point calibration protocol [56] and in accordance with the new IUPAC recommendation [57].

X-ray photoelectron spectroscopy (XPS) was used to identify the atmospheric corrosion products present at the surface of samples ZVI0 and ZVI8. Samples were mounted and analysed under high vacuum (<5 × 10<sup>-8</sup> mbar) in a Thermo VG Scientific X-ray photoelectron spectrometer (XPS) equipped with a dual anode X-ray source (Al Kα 1486.6 eV and Mg Kα 1253 eV). Al Kα radiation was used at 400 W (15 kV) and high resolution scans were acquired using a 30 eV pass energy, 0.1 eV step size and 200 ms dwell times.

## 4. Results and discussion

### 4.1. Expression of experimental results

Given that the initial rate of iron dissolution for each material was expected to follow a linear function ( $[\text{Fe}]_t = k_{\text{EDTA}}t + b$ ), regression of the experimental data (Fe concentration versus reaction time) allowed calculation of the linear dissolution function for each individual material. Direct comparison of the calculated rates of iron dissolution ( $k_{\text{EDTA}}$ ) could be used to indicate the more reactive ZVI materials, while the calculated intercept (' $b$ ') values could be used to indicate the relative amount of pre-existing corrosion products present on the material surfaces. To further characterize Fe<sup>0</sup>/EDTA systems, a new parameter is introduced ( $\tau_{\text{EDTA}}$ ). Per definition,  $\tau_{\text{EDTA}}$  for a given system is the time require for the iron concentration to reach 2 mM (112 mg L<sup>-1</sup>); that is the time to achieve saturation assuming 1:1 complexation of Fe<sup>II,III</sup> by EDTA. Thus,  $\tau_{\text{EDTA}}$  is the solution of the equation  $k_{\text{EDTA}}t + b = 112$ . The regression parameters of the experimental data are summarised in two tables (Table 2 and Table 3).

### 4.2. Qualitative XPS analysis

XPS results from analysis of materials ZVI0 and ZVI8 before experimental reaction clearly indicated that the uppermost surfaces of the two materials were iron oxide. The binding energy of the recorded Fe 2p lines was typical of Fe<sup>III</sup> in Fe<sub>2</sub>O<sub>3</sub> (hematite),

**Table 2**

Corresponding correlation parameters ( $k_{\text{EDTA}}$ ,  $b$ ,  $R$ ) and  $\tau_{\text{EDTA}}$  for the 18 metallic iron materials. As a rule, the more reactive a material is under given conditions the bigger the  $k_{\text{EDTA}}$  value or the smaller  $\tau_{\text{EDTA}}$ . General conditions: initial pH 5.2, initial EDTA concentration 2 mM, room temperature  $23 \pm 2^\circ\text{C}$ , and  $\text{Fe}^0$  mass loading  $2 \text{ g L}^{-1}$ .  $n$  is the number of experimental points for which the curve iron vs. time is linear.  $k_{\text{EDTA}}$  and  $b$ -values were calculated in Origin 6.0.

$\text{Fe}^0$	$n$	$R$	$k_{\text{EDTA}} (\mu\text{g h}^{-1})$	$b (\mu\text{g})$	$\tau_{\text{EDTA}} (\text{day})$
ZVI7	4	0.992	$1.3 \pm 0.1$	$37 \pm 8$	192.8
ZVI8	5	0.999	$18 \pm 1$	$89 \pm 12$	13.4
ZVI9	5	1.000	$24.5 \pm 0.3$	$103 \pm 9$	9.8
ZVI17	6	0.993	$29 \pm 2$	$116 \pm 44$	7.8
ZVI5	6	0.995	$33 \pm 2$	$50 \pm 87$	7.1
ZVI0	6	0.996	$33 \pm 1$	$64 \pm 55$	7.0
ZVI11	6	0.995	$34 \pm 2$	$87 \pm 57$	6.9
ZVI10	5	0.996	$37 \pm 3$	$18 \pm 60$	6.3
ZVI1	4	0.978	$46 \pm 6$	$2280 \pm 331$	2.9
ZVI4	4	0.987	$51 \pm 5$	$241 \pm 112$	4.3
ZVI2	4	0.974	$53 \pm 6$	$2015 \pm 351$	2.8
ZVI3	4	0.980	$57 \pm 5$	$1758 \pm 281$	2.8
ZVI6	4	0.994	$57 \pm 6$	$382 \pm 208$	4.2
ZVI12	4	0.980	$70 \pm 15$	$1679 \pm 443$	2.5
ZVI14	4	0.995	$71 \pm 9$	$644 \pm 275$	2.6
ZVI13	4	0.995	$74 \pm 6$	$968 \pm 243$	2.7
ZVI15	3	0.993	$92 \pm 11$	$642 \pm 444$	2.2
ZVI16	3	0.996	$111 \pm 10$	$65 \pm 353$	2.1

although there was some evidence for a minor  $\text{Fe}^{\text{II}}$  oxide (magnetite/wüstite) component. No signal was recorded from the metal, indicating that the materials had a universal oxide coating of at least 10 nm equivalent to the maximum escape depth of photoelectrons from the sample. This result highlights, in agreement with the literature [30,58,59], the fact that most  $\text{Fe}^0$  materials will typically possess a surface oxide coating prior to their use in environmental applications. It has been shown that these coatings are rapidly removed from  $\text{Fe}^0$  surfaces upon immersion by an auto-reduction

**Table 3**

Corresponding correlation parameters ( $k_{\text{EDTA}}$ ,  $b$ ,  $R$ ) and  $\tau_{\text{EDTA}}$  of iron dissolution under various operational conditions. As a rule, the more reactive a material is under given conditions the bigger the  $k_{\text{EDTA}}$  or the smaller  $\tau_{\text{EDTA}}$ . General conditions: initial pH 5.2, initial EDTA concentration 2 mM, room temperature  $23 \pm 2^\circ\text{C}$ , and  $\text{Fe}^0$  mass loading  $2 \text{ g L}^{-1}$ . For the investigation of the effects of material pre-treatment a mass loading of  $5 \text{ g L}^{-1}$  was used. For each test item the used material is mentioned.  $n$  is the number of experimental points for which the curve iron vs. time is linear.  $k_{\text{EDTA}}$  and  $b$ -values were calculated in Origin 6.0. For orientation,  $n = 7$  corresponds to an experimental duration of 5 days in non-disturbed experiments (effects of metal loading and particle size).

Test items	Parameter	$n$	$R$	$k_{\text{EDTA}} (\mu\text{g h}^{-1})$	$b (\mu\text{g})$	$\tau_{\text{EDTA}} (d)$
Metal loading	$2 \text{ g L}^{-1}$	7	0.993	$15 \pm 1$	$46 \pm 10$	22.7
	$4 \text{ g L}^{-1}$	7	0.997	$21 \pm 1$	$79 \pm 19$	11.0
ZVI8	$8 \text{ g L}^{-1}$	7	0.997	$33 \pm 2$	$56 \pm 41$	10.2
	$16 \text{ g L}^{-1}$	7	0.989	$38 \pm 3$	$180 \pm 162$	5.9
	$32 \text{ g L}^{-1}$	7	0.984	$75 \pm 8$	$202 \pm 107$	4.6
	$64 \text{ g L}^{-1}$	7	0.978	$83 \pm 9$	$223 \pm 198$	4.0
$\text{Fe}^0$ particle size	0.0–0.125	5	0.986	$94 \pm 9$	$1914 \pm 222$	1.6
	0.125–0.200	5	0.990	$77 \pm 6$	$318 \pm 135$	2.9
ZVI4	0.2–0.315	5	0.993	$68 \pm 5$	$78 \pm 47$	3.4
	0.315–0.500	5	0.983	$61 \pm 6$	$138 \pm 128$	3.7
	0.500–1.00	7	0.985	$48 \pm 4$	$138 \pm 87$	4.7
	1.00–2.00	7	0.996	$27 \pm 1$	$33 \pm 14$	8.7
$\text{Fe}^0$ pre-treatment	None	9	0.988	$559 \pm 33$	$609 \pm 178$	0.79
	$\text{H}_2\text{O}$	9	0.983	$605 \pm 42$	$722 \pm 227$	0.72
ZVI8	Ascorbate	8	0.992	$863 \pm 44$	$594 \pm 178$	0.51
	EDTA	9	0.993	$626 \pm 28$	$366 \pm 148$	0.72
	HCl	9	0.996	$611 \pm 20$	$363 \pm 105$	0.74
Mixing type	None	10	0.996	$33.1 \pm 1.1$	$177 \pm 2$	13.9
	Sonification	4	0.989	$6154 \pm 637$	$1926 \pm 862$	0.1
ZVI0	Bubbling	9	0.995	$1237 \pm 48$	$340 \pm 58$	0.4
	Shaking	7	0.997	$218 \pm 19$	$1096 \pm 426$	1.9
Mixing intensity	$50 \text{ min}^{-1}$	7	0.988	$52 \pm 4$	$71 \pm 26$	3.7
	$150 \text{ min}^{-1}$	7	0.995	$192 \pm 9$	$264 \pm 77$	1.9
ZVI8	$200 \text{ min}^{-1}$	5	0.990	$898 \pm 72$	$758 \pm 204$	0.5
	$250 \text{ min}^{-1}$	4	0.995	$1070 \pm 79$	$415 \pm 182$	0.4

reaction [30,59]. Removed oxide layers (mostly  $\text{Fe}_2\text{O}_3$ ) are subsequently transformed to magnetite and green rust, which will not inhibit the process of contaminant reduction [30]. However, because reduction is not the fundamental contaminant removal mechanism in  $\text{Fe}^0/\text{H}_2\text{O}$  systems [16,17], it is still interesting to quantify the amount of oxide coatings.

#### 4.3. Effect of operational parameters

Among the tested materials ZVI4 (fillings) was one of the materials exhibiting the largest particle size distribution while exhibiting relative low proportion of fines. ZVI4 was resultantly used in investigations regarding the effects of particle size. Other parameter-testing experiments were conducted with ZVI8 or ZVI0. The preference for ZVI8 is justified by its spherical form, its minor dissolution reactivity ( $k_{\text{EDTA}}$  and  $\tau_{\text{EDTA}}$  in Table 2) and the fact that the material is rusted and could recover its metallic glaze only after HCl or EDTA washing. While using a less reactive material in experiments where reactivity enhancement is expected (e.g., metal loading, mixing intensity), a large window of opportunity is expected before solution saturation ( $[\text{Fe}] < 112 \text{ mg L}^{-1}$ ). The available surface area of ZVI8 was estimated using the relation  $S = 6/\rho d$  [60], where  $\rho$  is the density ( $7800 \text{ kg m}^{-3}$ ) of  $\text{Fe}^0$  and  $d$  the particle diameter ( $d = 1.2 \text{ mm}$ , Table SI 1).

##### 4.3.1. Effect of $\text{Fe}^0$ type

Eighteen types of  $\text{Fe}^0$  materials (Tables SI 1 and SI 2) were evaluated using the EDTA dissolution method described (type 1 open system). The calculated dissolution rates ( $k_{\text{EDTA}}$ ) are displayed in Table 2 and vary from 1.3 to  $111 \mu\text{g h}^{-1}$ . The large range in reactivity ratios recorded for the materials indicates variability in reactivity between the  $\text{Fe}^0$  materials. The most reactive material was ZVI

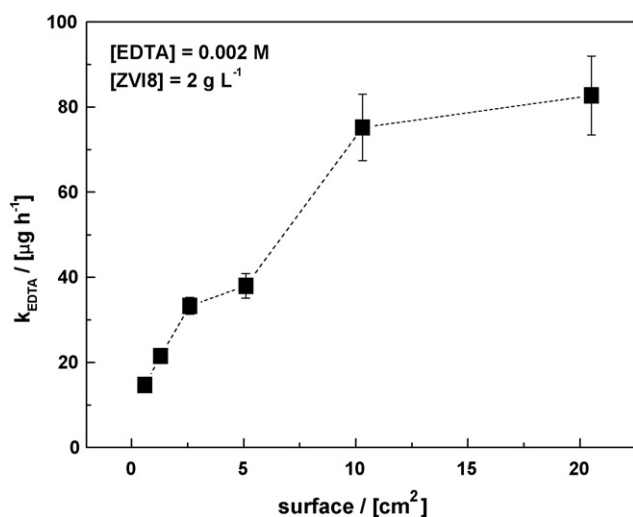


Fig. 1. Variation of the rate of iron dissolution ( $k_{\text{EDTA}}$ ) as a function of available  $\text{Fe}^0$  surface for the material ZVI8. The represented lines are not fitting functions, they just joint the points to facilitate visualization.

16 ( $\tau_{\text{EDTA}} = 2.1d$ ) displaying a dissolution rate of  $111 \mu\text{g h}^{-1}$ . Scrap iron sample ZVI7 displayed the lowest dissolution rate ( $1.3 \mu\text{g h}^{-1}$ ) indicating extremely limited reactivity. The intrinsic difference in the reactivity of various  $\text{Fe}^0$  materials may be considered as a significant source for controversial and variable results observed in the literature [18,19].

The general reactivity trend based on the material form was: powder > fillings > granular. Table 2 shows that some powders (ZVI1, ZVI2, ZVI3) are less reactive than ZVI6 (fillings). This result is mostly justified by the agglomeration of powders under the experimental conditions (non-shaken). Therefore, the EDTA-test may not be appropriate for some powdered materials ( $d < 0.1 \text{ mm}$ ). The results with ZVI15 (finer grade), ZVI16 (medium grade) and ZVI17 (coarser grade) from Connelly-GPM, Inc. demonstrated that large amounts of fines yield to increased but meaningless  $b$  values. Being from the same manufacturer, the three materials have the same chemical composition. Because these materials were used “as received” the observed high  $b$  values can be attributed to the proportion of fines.

#### 4.3.2. Effect of metal loading

The effect of the amount of ZVI8 on iron dissolution in 2 mM EDTA was investigated. The material was pre-washed in 50 mL of a 0.25 M HCl for 14 h to remove surface corrosion products and minimize their subsequent interference. It was found that the rate of iron dissolution increased as the amount of  $\text{Fe}^0$  was increased from 2 g to  $64 \text{ g L}^{-1}$  (or  $12\text{--}410 \text{ cm}^2 \text{ L}^{-1}$ ) (Table 3). However, the increase in iron dissolution rates was not linearly proportional to the increase in the amount of  $\text{Fe}^0$  reacted (Fig. 1). For amounts of material  $\leq 16 \text{ g L}^{-1}$  the observed dissolution rates increased at a linear rate with increasing metal loading ( $R = 0.943$ ) and a normalized iron dissolution rate of  $6.2 \mu\text{g h}^{-1} \text{ cm}^{-2}$  was estimated. Dissolution rates recorded for metal loads  $> 16 \text{ g L}^{-1}$  did not increase at a linear rate. For a more reactive material (e.g., ZVI11) the linearity range would be expected to be lower than for ZVI8 i.e.,  $< 16 \text{ g L}^{-1}$ . In fact, the more reactive a material the more rapid the kinetics of iron dissolution and thus the shorter the time to solution saturation.  $16 \text{ g L}^{-1}$  metal load of ZVI8 corresponds to  $102 \text{ cm}^2 \text{ L}^{-1}$  available surface.

The surface normalized reaction constant ( $k_{\text{SA}}$ ) is frequently used in evaluating kinetic data from elemental iron reactions and in comparing iron reactivity toward various classes of compounds [51]. The key relationship behind the normalization procedure is

linear proportionality between the rate constants and metal loading. There has been controversy over validity of  $k_{\text{SA}}$  for normalizing the rate constants by metal loading ([21,61,62] and references therein). The results above show that for ZVI8 and under non-shaken conditions linearity is observed only for  $[\text{ZVI}] \leq 16 \text{ g L}^{-1}$  ( $102 \text{ cm}^2 \text{ L}^{-1}$ ). It should be emphasized that mixing will lower this critical mass loading for ZVI8 because of accelerated transport of molecular  $\text{O}_2$  to the  $\text{Fe}^0$  surface. The large majority of experiments are conducted under mixing conditions and with larger metal loadings. Therefore, the reported significant variations among  $k_{\text{SA}}$  data (even for a given compound) are difficult to interpret. In the future this comparison should be eased by routinely given  $\tau_{\text{EDTA}}$  for each experimental condition.

It is interesting to note that a certain linearity trend of  $b$  value as function of mass loading was observed ( $R = 0.854$ ). This linear dependence of  $b$  values from the metal loading validates the enounced signification of that parameter. In this experiment corrosion products resulted from the air oxidation of  $\text{Fe}^0$  during the time elapsed between stopping HCl washing and initiating EDTA dissolution. Therefore, the corrosion products did not have time to precipitate and/or crystallize. As shown above (XPS results),  $\text{Fe}^0$  materials are covered with amorphous and crystalline iron oxides with differential dissolution behaviour. For granular materials as ZVI8, it is assumed that the dissolution of iron oxide in EDTA is more favourable than the oxidative dissolution of  $\text{Fe}^0$  from the material. This assumption is the support of the significance of  $b$  values and could be verified for ZVI0 and ZVI8 used in parallel “as received”, 2 mM EDTA-washed, and 250 mM HCl-washed experiments [32]. For materials with large amounts of fines (e.g., powdered materials and ZVI16/ZVI17), however,  $b$  values were proven meaningless. Because  $k_{\text{EDTA}}$  and  $b$  values are used to calculate  $\tau_{\text{EDTA}}$ , erroneous  $b$  values have an incidence on the validity of  $\tau_{\text{EDTA}}$ . Therefore, the EDTA-test should be limited to coarser material ( $d > 150 \mu\text{m}$ ). Alternatively,  $\text{Fe}^0$  materials can be compared on the basis of extent of leached Fe in column studies (e.g., starting from 1 g of each material). In column studies saturation is not expected and the differential dissolution of  $\text{Fe}^0$  and Fe-oxide can be better characterized.

The comparison of  $k_{\text{EDTA}}$  and  $\tau_{\text{EDTA}}$  values (Table 3) for the individual metal loadings shows that reactivity increased 6 fold as the metal loading varies from 2 to  $64 \text{ g L}^{-1}$ . Considering that essentially higher metal loadings (up to  $200 \text{ g L}^{-1}$  and more) are used by several researchers another discrepancy source is identified.

As discussed above higher metal loadings are directly related to more iron oxides generation, that are more adsorption sites for all contaminants, including metals and radionuclides. Therefore, in investigating the process of contaminant removal by  $\text{Fe}^0$  materials, the less possible metal loading should be used [62]. Considering that ZVI8 contains 92% Fe, the molar ratio Fe:EDTA varies from 1 to 26 as the mass loading varies from 2 to  $64 \text{ g L}^{-1}$ . This result shows that, apart from the experiment with  $2 \text{ g L}^{-1}$ ,  $\text{Fe}^0$  was available in excess. Characterizing the availability of Fe from the metal structure is a part of this study (see Section 4.3.1) but using over proportional material excess complicates mechanistic investigations for example. For instance, a lag time (induction time) was reported in the process of contaminant removal by  $\text{Fe}^0$  materials [3]. This study shows that the initial iron dissolution is always fast. Therefore, the reported lag time is possibly the time necessary for enough iron oxides to precipitate and adsorb contaminants. Adsorbed contaminants can be further transformed, e.g., reduced by: (i) dissolved  $\text{Fe}^{\text{II}}$ , (ii) oxide-bounded  $\text{Fe}^{\text{II}}$ , (iii) atomic (H) or molecular ( $\text{H}_2$ ) hydrogen.

#### 4.3.3. Effect of $\text{Fe}^0$ particle size

The effect of  $\text{Fe}^0$  particle size on the iron dissolution in 2 mM EDTA was investigated using ZVI4. The material was sieved into six particle fractions (Table 3) and an equal mass of each was reacted.

The results show increased rates of iron dissolution (increasing  $k_{\text{EDTA}}$  or decreasing  $\tau_{\text{EDTA}}$ ) with decreasing particle size. The evolution of the curve  $\tau_{\text{EDTA}} = f(d)$  (not shown) suggests that according to particle size, three ranges of reactivity can be distinguished: (i) very reactive ( $d \leq 0.2$  mm,  $\tau_{\text{EDTA}} < 3d$ ) corresponding to linear increasing of  $\tau_{\text{EDTA}}$  with increasing  $d$ ; (ii) fairly reactive ( $0.2 \leq d(\text{mm}) \leq 0.8$ ,  $3 < \tau_{\text{EDTA}} (d) < 5$ ), corresponding to a plateau in the variation  $\tau_{\text{EDTA}}$  with  $d$ ; and (iii) less reactive ( $0.8 \leq d(\text{mm}) \leq 2.0$ ,  $\tau_{\text{EDTA}} > 5d$ ). This classification suggests that only materials of similar particle sizes should be used in comparative investigations. Based on experimental results it is recommended that for testing micro-scale  $\text{Fe}^0$  materials with the EDTA method only particle diameters between 0.1 and 1.0 mm should be tested, ensuring that fines ( $d \leq 0.1$  mm) are separated by sieving (or washing).

The comparison of  $k_{\text{EDTA}}$  and  $\tau_{\text{EDTA}}$  values for the individual particle sizes shows that dissolution rate significantly decreases as the particle size was varied from  $\leq 0.125$  to 2.0 mm. This increase of reactivity with decreasing particle size is the rational of using nanoscale  $\text{Fe}^0$  for environmental remediation [60].

#### 4.3.4. Effect of material pre-treatment

The effect of material pre-treatment was investigated in open systems with a metal loading of  $5 \text{ g L}^{-1}$ . Four different pre-treatment procedures were tested. Pre-treatment consisted of washing 0.5 g of ZVI in 50 mL treatment solution for 14 h. The treatment solutions included: (i) deionised water (as a reference system), (ii) 0.115 M ascorbate buffer, (iii) 0.02 M EDTA, and (iv) 0.25 M HCl. The  $\text{Fe}^0$  samples were then rinsed three times with 50 mL deionised water before dissolution testing. The results presented in Table 3 showed that all pre-treatment procedures enhanced the reactivity of ZVI8. The observed iron dissolution rate varied from  $560 \mu\text{g h}^{-1}$  for the reference system to  $860 \mu\text{g h}^{-1}$  for the  $\text{Fe}^0$  system washed in 0.115 M ascorbate buffer. Calculated  $\tau_{\text{EDTA}}$  values confirmed that the greatest dissolution rate occurred in the ascorbate-treated system. It should be noted that the amount of solid material lost to dissolution during the pre-treatment procedure was not measured in this work. Previously, Matheson and Tratnyek [2] reported a 15% loss of iron mass during acid pre-treatment (3 h in 3% HCl), while  $\text{Fe}^0$  washing at neutral pH with ascorbate buffer was found exclusively to dissolve surface corrosion products, leaving a fresh residual  $\text{Fe}^0$  surface. Based on the current results it is suggested that ascorbate pre-treatment is a preferable procedure for removing surface corrosion from  $\text{Fe}^0$  materials than HCl washing which has previously been more commonplace.

While the effects of pre-treatment generally followed expectation (reactivity enhancement) the relevance of these procedures should be brought into question because  $\text{Fe}^0$  materials used in reactive barriers are not commonly pre-treated prior to emplacement [63]. Even if materials were pre-treated before emplacement surface oxides would rapidly form, long before any significant quantity of contaminant inflow [20,64].

#### 4.3.5. Effect of mixing

In investigating contaminant removal by  $\text{Fe}^0$  materials, sample mixing (mostly stirring or shaking) is commonly used as a tool for increasing the rate of reaction. For an inert material as activated carbon, mixing may have little or no effect on material reactivity. However, the thermodynamic instability of metallic iron ( $\text{Fe}^0$ ) in aqueous solution [2,65] is the primary reason for using elemental iron materials for groundwater remediation.

In undisturbed systems in the absence of EDTA, it is generally accepted that decreased  $\text{Fe}^0$  reactivity observed at pH > 5 is coupled to increased iron precipitation. However, a system which is physically disturbed by mixing will exhibit even greater  $\text{Fe}^0$  reactivity because the vigorous hydrodynamic conditions (turbulent

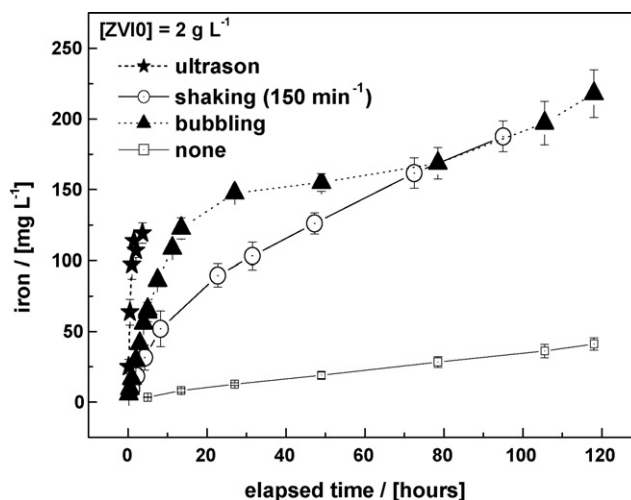


Fig. 2. Effects of the mixing type on the iron dissolution in 0.002 M EDTA. Bubbling and non-disturbed experiments were conducted under atmospheric partial pressure of  $\text{O}_2$  (open system). Shaking and ultrasound mixing experiments were conducted in closed systems. The represented lines are not fitting functions, they just joint the points to facilitate visualization.

flow) increase the rate and amount of iron dissolution/oxidation by: (i) breaking apart and subsequently preventing the aggregation of colloidal iron oxide and oxyhydroxide particles; (ii) continually exposing fresh  $\text{Fe}^0$  material through fragment collisions that dislodge and/or remove corrosion products from the material surface, and (iii) causing enhanced oxygen entrainment (diffusion) from the laboratory atmosphere into solution, thereby increasing rates of oxidation. Mixing will also facilitate transport of contaminants and reactive species to the  $\text{Fe}^0$  surface although in some cases contaminant desorption may be promoted [66].

In this section the effect of mixing on  $\text{Fe}^0$  dissolution is presented. Experiments were performed with two materials (ZVI0 and ZVI8) and three mixing types (bubbling, sonification and shaking).

4.3.5.1. *Effect of mixing type.* Fig. 2 summarises the effect of mixing type on the reactivity of ZVI0, the regression parameters and  $\tau_{\text{EDTA}}$  are given in Table 3. The results clearly indicate that all types of sample mixing enhance  $\text{Fe}^0$  reactivity. The dissolution rate varied from  $33 \mu\text{g h}^{-1}$  for the non-mixed system to  $6154 \mu\text{g h}^{-1}$  for the ultrasonically mixed system, which displayed the most rapid rate of iron dissolution. This result clearly show that while using different mixing devices and performing the experiments for the same duration (e.g., 4 h) various extents of  $\text{Fe}^0$  dissolution was achieved yielding to various amounts of contaminant removal agents ( $\text{Fe}^{\text{II}}$ ,  $\text{H}_2$ , Fe-oxides). Characterizing each experimental procedure with  $\tau_{\text{EDTA}}$  will certainly facilitate the discussion of achieved results.

4.3.5.2. *Effect of shaking intensity.* The effect of shaking intensity was investigated with ZVI8 for four different shaking rates: 50, 150, 200 and  $250 \text{ min}^{-1}$ . The results are summarised in Table 3 and follow theoretical predictions of enhanced dissolution behaviour with increasing mixing intensity.  $\tau_{\text{EDTA}}$  varied from 3.7 days for a mixing intensity of  $50 \text{ min}^{-1}$  to 0.4 days for  $250 \text{ min}^{-1}$ . The effect of shaking intensity is presented in more details elsewhere [43]. The results disprove the popular assumption that mixing batch experiments is a tool to limit or eliminate diffusion as dominant transport process of contaminant to the  $\text{Fe}^0$  surface.

4.3.5.3. *Discussion.* Ultrasonic vibration and solution shaking involved the physical movement of both solution and  $\text{Fe}^0$  mate-

rials. By comparison, solutions mixed by air bubbling left the Fe<sup>0</sup> material immobile while homogenising the overlying solution.

The ‘bubbled’ metal-solution system recorded a 40 fold enhancement in reactivity compared to the non-disturbed system. The bubbling maintained a continuously replenished supply of dissolved oxygen to the solution, promoting Fe<sup>0</sup> oxidation and yielding dissolved Fe<sup>II</sup> and Fe<sup>III</sup> which then complexed with EDTA. Results indicated a rapid initial dissolution rate for the first 10–15 h (Fig. 2) which subsequently tailed off by 80 h, showing a slight increase again to 120 h. The observed tail-off in dissolution rate occurred after iron saturation ( $[Fe] > 112 \text{ mg L}^{-1}$ ) had been reached and can be attributed to iron oxide nucleation and precipitation. Bubbling supplied the system with unrealistic amounts of dissolved O<sub>2</sub> which was unrealistic with regard to subsurface reactive walls. These conditions are encountered in above ground plant for wastewater treatment for which the Fe<sup>0</sup>/H<sub>2</sub>O system are also used [14].

Previous studies have found that sample agitation can disturb, delay or even prevent iron oxide precipitation at the Fe<sup>0</sup> surface [15,16,66]. Such mixing may allow contaminant transport to the Fe<sup>0</sup>/H<sub>2</sub>O interface, an interface which cannot exist in nature [24,62,64]. On this basis it can be argued that sample mixing and agitation may yield unrealistic results and should therefore be avoided when testing the reactivity of Fe<sup>0</sup> materials for commercial use in reactive barriers [18,19]. Note that all types of mixing devices can be used for above ground water treatment systems using Fe<sup>0</sup>. However, for subsurface applications, mixing should not significantly disturb the dynamic process of oxide-film formation and transformation.

Although the results have shown that Fe<sup>0</sup> reactivity and dissolution may be enhanced by elevated mixing intensities, the mixing process is also known to have an effect on iron oxide precipitation. It is well accepted that contaminants (including EDTA, see ref. [49]) can be entrapped in the matrix of precipitating iron oxides (co-precipitation). Typically, contaminant removal enhanced by mixing is considered to operate on the basis of maintaining a continual supply of freshly exposed Fe<sup>0</sup> surfaces for contaminant uptake. However, it is entirely possible that their co-precipitation with iron oxide may provide a competing removal mechanism. Even though co-precipitated contaminants can be further reduced by structural Fe<sup>II</sup> or atomic and molecular hydrogen (H, H<sub>2</sub>), the reaction cannot quantitatively occur at the Fe<sup>0</sup> surface as commonly reported.

The effect of the mixing intensity on Fe<sup>0</sup> reactivity confirms theoretical predictions but the discussion above questioned the validity of mixing to accelerate contaminant transfer to the Fe<sup>0</sup> surface. It is possible that a critical value exists below which mixing may have limited effect on oxide-film formation (e.g., 40 min<sup>-1</sup> in [20] or 50 min<sup>-1</sup> in [43]). However, mixing always increases iron dissolution and the Fe<sup>0</sup> surface is permanently covered with corrosion products. Therefore, it may be advantageous to conduct initial work under stagnant conditions and progressively increase the mixing intensity to discover which mixing speeds can be used without major iron precipitation interference [19]. Clearly, works investigating the same process can only be comparable if conducted under similar  $\tau_{\text{EDTA}}$  conditions.

## 5. Concluding remarks

The current study aimed at developing a reliable method for comparing and characterising different Fe<sup>0</sup> materials under various experimental conditions. For this purpose an aqueous dissolution method utilizing a dilute 0.002 M EDTA solution was adopted for the experimental work. Results showed that: (i) iron dissolution in non-disturbed experiments is a powerful tool for material screening; (ii) mixing type, mixing intensity, particle size and Fe<sup>0</sup> loading

enhance the material reactivity to various extents. In particular, material pre-treatment, too rapid mixing speeds or too high Fe<sup>0</sup> dosages may yield reproducible but non-realistic results. Since the investigated parameters are not independent from each other it was necessary to introduce a parameter ( $\tau_{\text{EDTA}}$ ) which allows a reliable characterization of Fe<sup>0</sup> reactivity under each experimental condition. Therefore, similar to iodine number for activated carbon,  $\tau_{\text{EDTA}}$  is introduced to characterise material reactivity. Ideally, any work with Fe<sup>0</sup> should specify  $\tau_{\text{EDTA}}$  under the experimental conditions. However, despite its practical simplicity,  $\tau_{\text{EDTA}}$  is an extrapolation which accuracy depends on the amount of corrosion products on original materials ( $b$  values). Therefore,  $k_{\text{EDTA}}$  is a better parameter to characterize the reactivity of each Fe<sup>0</sup>.

While literature on Fe<sup>0</sup> remediation predominantly assumes that contaminant removal mostly occurs through electrochemical reduction at the surface of Fe<sup>0</sup> materials, the results of this study and related works [18,19,43,62] indicated that under environmental conditions contaminant removal may primarily occur in conjunction with the dynamic process of precipitation of corrosion products (non-selective process). The first proof for this statement is that Fe<sup>0</sup>/H<sub>2</sub>O systems have efficiently reduced some contaminants, oxidized some others, and even removed some redox-insensitive contaminants [9,10,46]. Therefore, oxidation and reduction should be regarded as subsequent processes in the presence of immersed corroding Fe<sup>0</sup> (statement 1). The concept regarding adsorption and co-precipitation as fundamental contaminant removal mechanisms in Fe<sup>0</sup>/H<sub>2</sub>O system is based on statement 1. This concept has partly faced with very sceptic views [67,68]. For example, The authors of ref. [68] complained that this concept “is hardly acceptable since the role of the direct electron transfer in ZVI-mediated reactions is well established and generally accepted among the research community.” However, the well-accepted “role of direct electron transfer in ZVI-mediated reactions” was demonstrably a “broad consensus” as recognized by O’Hannesin and Gillham [4]. On the other hand, the authors of [67] were “mystified” by any possible convergence between the mechanism of uranium (U) and an organohalide in Fe<sup>0</sup>/H<sub>2</sub>O systems because “the topic of U(VI) reduction is clearly remote from that of organohalide reduction”. These two examples illustrate the difficulty in revising a well established but inconsistent concept. Fortunately, electrocoagulation (EC) using iron electrodes (Fe<sup>0</sup> EC) is rigorously an electrochemically accelerated iron corrosion and has proven similar efficiency as passive Fe<sup>0</sup>/H<sub>2</sub>O systems for the removal of various chemical contaminants and pathogens [69–71]. For Fe<sup>0</sup> EC no one has suggested Fe<sup>0</sup> electrodes as reducing agents, because Fe<sup>0</sup> is intentionally corroded to produce “flocs” for contaminant co-precipitation. The similarity between passive Fe<sup>0</sup>/H<sub>2</sub>O systems and Fe<sup>0</sup> EC should convince the last sceptics. The scientific community will then concentrate on the further development of the technology.

Interestingly, the scientific community is on schedule to identify the “common underlying mechanisms for reactions” in iron walls that provide a confidence for non-site-specific design. Is this the case, then “site-specific treatability studies may only be required to fine-tune design criteria for the optimal performance of PRBs” [72]. The concept of contaminant adsorption/co-precipitation can be regarded as the first step to this goal. The scientific community should abandon the current approach which merit was to demonstrate the efficiency of Fe<sup>0</sup> for several contaminants (and groups of contaminants). The challenge now is to incorporate future studies within a broad-based understanding of Fe<sup>0</sup> remediation technology. In particular, the removal mechanism of individual contaminants by Fe<sup>0</sup> materials has to be investigated under non-disturbed conditions and with realistic metal loadings. The proper use of  $\tau_{\text{EDTA}}$  and  $k_{\text{EDTA}}$  is a precious guide on this high way.

## Acknowledgments

For providing the materials investigated in this study the authors would like to express their gratitude to the branch of the MAZ (Metallaufbereitung Zwickau, Co) in Freiberg (Germany), Gotthart Maier Metallpulver GmbH (Rheinfelden, Germany), Connelly-GPM Inc. (USA), Dr. Ralf Köber from the Institute Earth Science of the University of Kiel and Dr. Vera Biermann from the Federal Institute for Materials Research and Testing (Berlin, Germany), Mechthild Rittmeier and Rüdiger Pfaar are acknowledged for technical support. The manuscript was improved by the insightful comments of anonymous reviewers from Journal of Hazardous Materials. The work was granted by the Deutsche Forschungsgemeinschaft (DFG-No 626/2-1).

## Appendix A. Supplementary data

Supplementary data associated with this article can be found, in the online version, at doi:10.1016/j.jhazmat.2009.07.097.

## References

- [1] R.W. Gillham, S.F. O'Hannesin, Enhanced degradation of halogenated aliphatics by zero-valent iron, *Ground Water* 32 (1994) 958–967.
- [2] L.J. Matheson, P.G. Tratnyek, Reductive dehalogenation of chlorinated methanes by iron metal, *Environ. Sci. Technol.* 28 (1994) 2045–2053.
- [3] C.G. Schreier, M. Reinhard, Transformation of chlorinated organic compounds by iron and manganese powders in buffered water and in landfill leachate, *Chemosphere* 29 (1994) 1743–1753.
- [4] S.F. O'Hannesin, R.W. Gillham, Long-term performance of an in situ "iron wall" for remediation of VOCs, *Ground Water* 36 (1998) 164–170.
- [5] T. Bigg, S.J. Judd, Zero-valent iron for water treatment, *Environ. Technol.* 21 (2000) 661–670.
- [6] D.W. Blowes, C.J. Ptacek, S.G. Benner, W.T. Mccrae Che, T.A. Bennett, R.W. Puls, Treatment of inorganic contaminants using permeable reactive barriers, *J. Contam. Hydrol.* 45 (2000) 123–137.
- [7] M.M. Scherer, S. Richter, R.L. Valentine, P.J.J. Alvarez, Chemistry and microbiology of permeable reactive barriers for in situ groundwater clean up, *Rev. Environ. Sci. Technol.* 30 (2000) 363–411.
- [8] J.L. Jambor, M. Raudsepp, K. Mountjoy, Mineralogy of permeable reactive barriers for the attenuation of subsurface contaminants, *Can. Miner.* 43 (2005) 2117–2140.
- [9] A.D. Henderson, A.H. Demond, Long-term performance of zero-valent iron permeable reactive barriers: a critical review, *Environ. Eng. Sci.* 24 (2007) 401–423.
- [10] A.B. Cundy, L. Hopkinson, R.L.D. Whitby, Use of iron-based technologies in contaminated land and groundwater remediation: a review, *Sci. Total Environ.* 400 (2008) 42–51.
- [11] R.L. Johnson, R.B. Thoms, R.O'B. Johnson, T. Krug, Field evidence for flow reduction through a zero-valent iron permeable reactive barrier, *Ground Water Monit. Remed.* 28 (2008) 47–55.
- [12] R. Thiruvenkatachari, S. Vigneswaran, R. Naidu, Permeable reactive barrier for groundwater remediation, *J. Ind. Eng. Chem.* 14 (2008) 145–156.
- [13] J. Suk, O.S.-W. Jeon, R.W. Gillham, L. Gui, Effects of initial iron corrosion rate on long-term performance of iron permeable reactive barriers: column experiments and numerical simulation, *J. Contam. Hydrol.* 103 (2009) 145–156.
- [14] T. Pradeep, Anshup, Noble metal nanoparticles for water purification: a critical review, *Thin Solid Films*, doi:10.1016/j.tsf.2009.03.195, in press.
- [15] L. Xie, C. Shang, The effects of operational parameters and common anions on the reactivity of zero-valent iron in bromate reduction, *Chemosphere* 66 (2007) 1652–1659.
- [16] C. Noubactep, Processes of contaminant removal in "Fe<sup>0</sup>-H<sub>2</sub>O" systems revisited: the importance of co-precipitation, *Open Environ. J.* 1 (2007) 9–13.
- [17] C. Noubactep, A critical review on the mechanism of contaminant removal in Fe<sup>0</sup>-H<sub>2</sub>O systems, *Environ. Technol.* 29 (2008) 909–920.
- [18] C. Noubactep, Characterizing the discoloration of methylene blue in Fe<sup>0</sup>/H<sub>2</sub>O systems, *J. Hazard. Mater.* 166 (2009) 79–87.
- [19] C. Noubactep, A.-M.F. Kurth, M. Sauter, Evaluation of the effects of shaking intensity on the process of methylene blue discoloration by metallic iron, *J. Hazard. Mater.* 169 (2009) 1005–1011.
- [20] S. Choe, Y.Y. Chang, K.Y. Hwang, J. Khim, Kinetics of reductive denitrification by nanoscale zero-valent iron, *Chemosphere* 41 (2000) 1307–1311.
- [21] H. Song, E.R. Carraway, Reduction of chlorinated methanes by nanosized zero-valent iron: kinetics, pathways and effects of reaction conditions, *Environ. Eng. Sci.* 23 (2006) 272–284.
- [22] P. Varanasi, A. Fullana, S. Sidhu, Remediation of PCB contaminated soils using iron nano-particles, *Chemosphere* 66 (2007) 1031–1038.
- [23] P. Westerhoff, J. James, Nitrate removal in zero-valent iron packed columns, *Water Res.* 37 (2003) 1818–1830.
- [24] V. Battaglia, J. Newman, Modeling of a growing oxide film: the iron/iron oxide system, *J. Electrochem. Soc.* 142 (1995) 1423–1430.
- [25] E.J. Caule, M. Cohen, The formation of thin films of iron oxide, *Can. J. Chem.* 33 (1955) 288–304.
- [26] M. Cohen, The formation and properties of passive films on iron, *Can. J. Chem.* 37 (1959) 286–291.
- [27] M. Stratmann, J. Müller, The mechanism of the oxygen reduction on rust-covered metal substrates, *Corros. Sci.* 36 (1994) 327–359.
- [28] A. Abdelouas, W. Lutze, H.E. Nutall, W. Gong, Réduction de l'U(VI) par le fer métallique: application à la dépollution des eaux, *C. R. Acad. Sci. Paris Earth Planet. Sci.* 328 (1999) 315–319.
- [29] J.-L. Chen, S.R. Al-Abed, J.A. Ryan, Z. Li, Effects of pH on dechlorination of trichloroethylene by zero-valent iron, *J. Hazard. Mater.* B83 (2001) 243–254.
- [30] K. Ritter, M.S. Odziemkowski, R.W. Gillham, An in situ study of the role of surface films on granular iron in the permeable iron wall technology, *J. Contam. Hydrol.* 55 (2002) 87–111.
- [31] E.M. Pierce, D.M. Wellman, A.M. Lodge, E.A. Rodriguez, Experimental determination of the dissolution kinetics of zero-valent iron in the presence of organic complexants, *Environ. Chem.* 4 (2007) 260–270.
- [32] C. Noubactep, M. Fall, G. Meinrath, B. Merkel, A simple method to select zero valent iron material for groundwater remediation, in: Paper presented at the Quebec 2004, 57th Canadian Geotechnical Conference, 5th Joint CGS/IAH-CNC Conference, Session 1A, 2004, pp. 6–13.
- [33] C. Noubactep, G. Meinrath, P. Dietrich, M. Sauter, B. Merkel, Testing the suitability of zerovalent iron materials for reactive walls, *Environ. Chem.* 2 (2005) 71–76.
- [34] J.S. LaLind, A.T. Stone, Reductive dissolution of goethite by phenolic reductants, *Geochim. Cosmochim. Acta* 53 (1989) 961–971.
- [35] J.E. Kostka, K.H. Nealson, Dissolution and reduction of magnetite by bacteria, *Environ. Sci. Technol.* 29 (1995) 2535–2540.
- [36] Y. Deng, Effect of pH on the reductive dissolution rates of iron(III) hydroxide by ascorbate, *Langmuir* 13 (1997) 1835–1839.
- [37] E.H. Oelkers, General kinetic description of multioxide silicate mineral and glass dissolution, *Geochim. Cosmochim. Acta* 65 (2001) 3703–3719.
- [38] N. Schuwirth, T. Hofmann, Comparability of and alternatives to leaching tests for the assessment of the emission of inorganic soil contamination, *J. Soils Sediments* 6 (2005) 1–11.
- [39] L.G.M. Baas-Becking, I.R. Kaplan, D. Moore, Limits of the natural environments in terms of pH and oxidation–reduction potentials, *J. Geol.* 68 (1960) 243–284.
- [40] E. Sada, H. Kumazawa, H. Machida, Oxidation kinetics of Fe<sup>II</sup>-EDTA and Fe<sup>II</sup>-NTA chelates by dissolved oxygen, *Ind. Eng. Chem. Res.* 26 (1987) 1468–1472.
- [41] S. Seibig, R. van Eldik, Kinetics of [Fe<sup>II</sup>(edta)] oxidation by molecular oxygen revisited. New evidence for a multistep mechanism, *Inorg. Chem.* 36 (1997) 4115–4120.
- [42] S. Bonneville, P. Van Cappellen, T. Behrends, Microbial reduction of iron(III) oxyhydroxides: effects of mineral solubility and availability, *Chem. Geol.* 212 (2004) 255–268.
- [43] C. Noubactep, Characterizing the effects of shaking intensity on the kinetics of metallic iron dissolution in EDTA, *J. Hazard. Mater.*, doi:10.1016/j.jhazmat.2009.05.085, in press.
- [44] C. Noradoun, M.D. Engelmann, M. McLaughlin, R. Hutcheson, K. Breen, A. Paszczynski, I.F. Cheng, Destruction of chlorinated phenols by dioxygen activation under aqueous room temperature and pressure conditions, *Ind. Eng. Chem. Res.* 42 (2003) 5024–5030.
- [45] C.E. Noradoun, C.S. Mekmaysy, R.M. Hutcheson, I.F. Cheng, Detoxification of malathion a chemical warfare agent analog using oxygen activation at room temperature and pressure, *Green Chem.* 7 (2005) 426–430.
- [46] D.F. Laine, I.F. Cheng, The destruction of organic pollutants under mild reaction conditions: a review, *Microchem. J.* 85 (2007) 183–193.
- [47] I. Sanchez, F. Stüber, J. Font, A. Fortuny, A. Fabregat, C. Bengoa, Elimination of phenol and aromatic compounds by zero valent iron and EDTA at low temperature and atmospheric pressure, *Chemosphere* 68 (2007) 338–344.
- [48] D.F. Laine, A. Blumenfeld, I.F. Cheng, Mechanistic study of the ZEA organic pollutant degradation system: evidence for H<sub>2</sub>O<sub>2</sub>, HO•, and the homogeneous activation of O<sub>2</sub> by Fe<sup>II</sup>EDTA, *Ind. Eng. Chem. Res.* 47 (2008) 6502–6508.
- [49] O. Gylie, T. Vengris, A. Stoncius, O. Nivinskien, Decontamination of solutions containing EDTA using metallic iron, *J. Hazard. Mater.* 159 (2008) 446–451.
- [50] J. Pietsch, W. Schmidt, F. Sacher, S. Fichtner, H. Brauch, Pesticides and another organic micropollutants in the river Elbe, *Fresenius J. Anal. Chem.* 353 (1995) 75–82.
- [51] T.L. Johnson, M.M. Scherer, P.G. Tratnyek, Kinetics of halogenated organic compound degradation by iron metal, *Environ. Sci. Technol.* 30 (1996) 2634–2640.
- [52] Y.H. Liou, S.-L. Lo, C.-J. Lin, W.H. Kuan, S.C. Weng, Effects of iron surface pretreatment on kinetics of aqueous nitrate reduction, *J. Hazard. Mater.* B126 (2005) 189–194.
- [53] S.M. Ponder, J.G. Darab, T.E. Mallouk, Remediation of Cr(VI) and Pb(II) aqueous solutions using supported, nanoscale zero-valent iron, *Environ. Sci. Technol.* 34 (2000) 2564–2569.
- [54] W.B. Fortune, M.G. Mellon, Determination of iron with o-phenanthroline: a spectrophotometric study, *Ind. Eng. Chem. Anal. Ed.* 10 (1938) 60–64.
- [55] L.G. Saywell, B.B. Cunningham, Determination of iron: colorimetric o-phenanthroline method, *Ind. Eng. Chem. Anal. Ed.* 9 (1937) 67–69.
- [56] G. Meinrath, P. Spitzer, Uncertainties in determination of pH, *Mikrochem. Acta* 135 (2000) 155–168.
- [57] R.P. Buck, S. Rondinini, A.K. Covington, F.G.K. Baucke, C.M.A. Brett, M.F. Camoes, M.J.T. Milton, T. Mussini, R. Naumann, K.W. Pratt, P. Spitzer, G.S. Wilson,

- Measurement of pH. Definition, standards, and procedures (IUPAC recommendations 2002), *Pure Appl. Chem.* 74 (2002) 2169–2200.
- [58] M. Stratmann, K. Hoffmann, In situ Mößbauer spectroscopic study of reactions within rust layers, *Corros. Sci.* 29 (1989) 1329–1352.
- [59] M.S. Odziemkowski, R.P. Simpraga, Distribution of oxides on iron materials used for remediation of organic groundwater contaminants – implications for hydrogen evolution reactions, *Can. J. Chem. Rev. Can. Chim.* 82 (2004) 1495–1506.
- [60] C. Macé, S. Desrocher, F. Gheorghiu, A. Kane, M. Pupeza, M. Cernik, P. Kvapil, R. Venkatakrishnan, W.-X. Zhang, Nanotechnology and groundwater remediation: a step forward in technology understanding, *Remediation* 16 (2006) 23–33.
- [61] C. Noubactep, On the validity of specific rate constants ( $k_{SA}$ ) in  $Fe^0/H_2O$  systems, *J. Hazard. Mater.* 164 (2009) 835–837.
- [62] C. Noubactep, An analysis of the evolution of reactive species in  $Fe^0/H_2O$  systems, *J. Hazard. Mater.* 168 (2009) 1626–1631.
- [63] C. Noubactep, P. Volke, B. Merkel, G. Meinrath, Mitigation of uranium in effluents by zerovalent iron: the role of iron corrosion products, in: *International Conference on Radioactive Waste Management and Environmental Remediation*, 8th. 2001, Bruges, Belgium, 2001, American Society of Mechanical Engineers.
- [64] T.B. Scott, G.C. Allen, P.J. Heard, M.G. Randell, Reduction of U(VI) to U(IV) on the surface of magnetite, *Geochim. Cosmochim. Acta* 69 (2005) 5639–5646.
- [65] E.R. Wilson, The mechanism of the corrosion of iron and steel in natural waters and the calculation of specific rates of corrosion, *Ind. Eng. Chem.* 15 (1923) 127–133.
- [66] N.D. Tomashov, L.P. Vershinina, Kinetics of some electrode processes on a continuously renewed surface of solid metal, *Electrochim. Acta* 15 (1970) 501–517.
- [67] M. Elsner, D.M. Cwiertny, A.L. Roberts, B.S. Lollar, Response to comment on “1,1,2,2-tetrachloroethane reactions with  $OH^-$ , Cr(II), granular iron, and a copper-iron bimetal: insights from product formation and associated carbon isotope fractionation”, *Environ. Sci. Technol.* 41 (2007) 7949–7950.
- [68] S.-H. Kang, W. Choi, Response to comment on “oxidative degradation of organic compounds using zero-valent iron in the presence of natural organic matter serving as an electron shuttle”, *Environ. Sci. Technol.* 43 (2009) 3966–3967.
- [69] M.Y.A. Mollah, R. Schennach, J.R. Parga, D.L. Cocke, Electrocoagulation (EC) – science and applications, *J. Hazard. Mater.* 84 (2001) 29–41.
- [70] D. Lakshmanan, D.A. Clifford, G. Samanta, Ferrous and ferric ion generation during iron electrocoagulation, *Environ. Sci. Technol.* 43 (2009) 3853–3859.
- [71] C.H.A. Moreno, D.L. Cocke, J.A.G. Gomes, P. Morkovsky, J.R. Parga, E. Peterson, C. Garcia, Electrochemical reactions for electrocoagulation using iron electrodes, *Ind. Eng. Chem. Res.* 48 (2009) 2275–2282.
- [72] K.L. McGeough, R.M. Kalin, P. Myles, Carbon disulfide removal by zero valent iron, *Environ. Sci. Technol.* 41 (2007) 4607–4612.